Microstructure Effect of an Alumina-forming Duplex Stainless Steel on High-temperature Steam Oxidation

Woong Heo, Chaewon Kim, Changheui Jang*
Korea Advanced Institute of Science and Technology, Daejeon, Korea
**Corresponding author: chjang@kaist.ac.kr*

1. Introduction

After the Fukushima accident in March 2011, it is demanded to enhance accident tolerance in the nuclear industry. Accordingly, there has been a lot of research on the development of accident tolerant fuel (ATF) cladding. As a candidate for ATF cladding, Fe-base alloys are under consideration. Especially, FeCrAl alloys are actively studied because of superior high-temperature oxidation resistance. But, there are also challenges for using FeCrAl alloys as a cladding like a thin tube fabrication, thermal aging, etc [1, 2]. Recently, alumina-forming duplex stainless steels (ADSS) were developed as an ATF cladding material. ADSS alloys have not only superior high-temperature oxidation resistance but also high strength and reasonable ductility [3], which enables easier thin tube fabrication. The detailed information on ADSS alloys can be found in the previous studies [3-5].

ADSS alloys have a duplex structure with B2-NiAl precipitates. Phase fraction and distribution of precipitates are quite different depending on thermo mechanical process (TMP). For better properties, development of optimized TMP is needed and the microstructure effect on required properties should be evaluated. In this study, high-temperature steam oxidation behavior of ADSS #B51 with selected microstructures was evaluated. Finally, the microstructure effect of ADSS on high-temperature oxidation resistance will be discussed.

2. Materials and Experiments

2.1. Materials and microstructures

The ADSS #B51 with different microstructures and commercial FeCrAl alloy (Khantal APM), were used in this study. A 50 kg cast ingot of ADSS #B51 was made by vacuum induction melting (VIM). The ingot was applied homogenization heat treatment (HT) at 1200 °C for 4 h. Then, the ingot was hot rolled with a thickness reduction of 90 % followed by intermediate heat treatment. Subsequently, cold rolling with a thickness reduction of 40 % was applied to simulate thin tube fabrication and then final heat treatment was applied. The chemical composition of ADSS #B51 was analyzed by inductively coupled plasma atomic emission spectroscopy (ICP-AES) and the result are summarized in Table I with a chemical composition of APM to compare steam oxidation behavior.

To evaluate the microstructure effect of ADSS on high-temperature oxidation resistance, three plates of ADSS #B51 with different microstructures were used in this study. Figure 1 shows the selected microstructures of ADSS #B51. Such different microstructures are obtained by changing the temperature of hot rolling, intermediate heat treatment, and final heat treatment in TMP. In Fig. 1(a), the microstructure of #B51 after homogenization HT has ferrite with very fine B2-NiAl precipitates and austenite without B2 precipitate. After TMP, the microstructure of #B51 changes to Microstructure I~III shown in Fig. 1(b) ~ (d) and each different microstructure results from different TMP. Microstructure I has similar size and distribution of B2 precipitates in both austenite and ferrite. In Microstructure II, it seems to have coarsened and less B2 precipitates in the austenite compared to Microstructure I. In the ferrite of Microstructure II, there are coarsened B2 precipitates and very fine B2 precipitates. In microstructure III, there are fine B2 precipitates in ferrite and very small needle-like B2 precipitates in austenite.

2.2. High-temperature steam oxidation test

For high-temperature oxidation test, coupon-type specimens with a diameter of 15 mm, a thickness of 0.7 mm, and a hanging hole with a diameter of 1 mm were fabricated by electro discharge machining (EDM). Both sides of coupon specimens were ground using 1200-grit silicon carbide paper and ultrasonically cleaned in ethanol prior to the oxidation test.

Table I. Chemical composition of materials used in this study (in wt.%)

	Fe	Ni	Cr	Al	Nb	Mn	C	Si	Else
ADSS #B51	Bal.	19.29	15.88	6.23	0.19	1.02	0.108	0.33	
APM	Bal.	0.15	21.99	5.81	0.0029	0.16	0.033	0.28	Ti 0.038 Cu 0.023 Zr 0.15

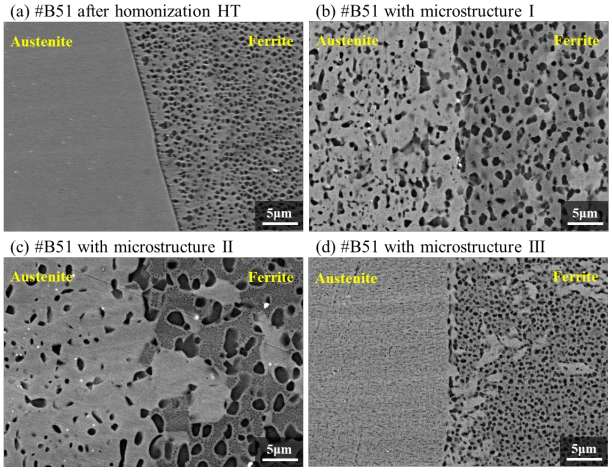

Figure 1. SEM (BSE) images of #B51 (a) after homogenization HT and (b)-(d) with microstructures I-III

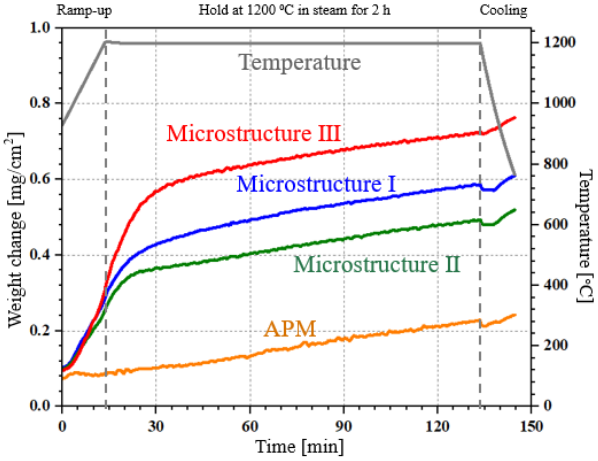

Figure 2. Steam TGA results at 1200 ºC for 2 h

For high-temperature oxidation test, the steam thermogravimetric analysis (TGA) system (STA 449 F2) was used at 1 bar. The coupon specimen was hanging to an alumina crucible by a Pt wire and loaded to test zone. The test zone was filled with Ar gas and heated to 600 ºC. Then, a mixture of steam and Ar was introduced to the test zone with a flow rate of 2 g/h. Then, the test zone heated to a target temperature of 1200 ºC with a heating rate of 20 K/min. After the temperature of the specimen reached 1200 ºC, test condition was maintained for 2 h. While the test was conducted, weight of the specimen was measured in real time using TGA system. For analysis of oxide and substrate, field emission scanning electron microscope (FE-SEM, SU8230, Hitachi) equipped with energy dispersive X-ray spectroscope (EDS) and X-ray diffractometry (XRD, D/MAX-2500, Rigaku) were used.

3. Results and discussion

Figure 2 shows steam TGA results of APM and three types of #B51. They all show very low weight gain. Among test materials, APM shows the lowest weight gain. For #B51, they showed a relatively fast oxidation rate with transient oxidation behavior in the early stage, and then reached steady-state oxidation with a slow oxidation rate. After the transient oxidation stage, #B51 and APM show a similar oxidation rate. It may result from the formation of protective alumina on #B51 and APM [3]. For the oxidation of three types of #B51, they have somewhat different weight gain graphs although they have the same chemical composition. Microstructure III shows 1.22 times higher weight gain than the microstructure I and 1.47 times higher than the microstructure II. Considering similar oxidation rate in latter steady-state oxidation region, difference in weight gain of three type of #B51 came from early oxidation behavior and it would be related to different microstructures.

SEM images (SE) of surface oxide formed after oxidation test were shown in Fig. 3. While only Al rich oxide was formed on APM, two types of oxides were found on #B51 after the steam oxidation tests. One is a ridge shape Al-rich oxide and the other is a nodular Fe, Cr, Al-rich oxide. Generally, it was reported that α-alumina has the ridge shape [6]. For ADSS alloys, spallation was observed regardless of microstructures and it was indicated in Fig. (c), (d).

XRD results after the oxidation test were shown in Fig. 4. Considering both SEM/EDS results and XRD results, only protective alpha alumina formed on APM and it results in the lowest weight gain of APM. For ADSS #B51, α-alumina and spinel type oxides are formed after the oxidation test. In addition, a continuous α-alumina layer was also formed below spinel oxides (It is not shown here). Therefore, the relatively fast oxidation rate of ADSS alloys in early stage results from the formation of spinel oxides. After continuous alpha alumina was formed below spinel oxides, they showed the slow oxidation rate.

Comparing the different microstructures of ADSS #B51, microstructure III exhibited the highest spinel peaks, middle in microstructure I, and lowest in microstructure II. This trends of relative quantities of spinel oxides were well matched to steam TGA results. Therefore, the formation of spinel oxides mainly affects fast oxidation rate of ADSS alloys in early stage and the amount of spinel oxides depends on the existing microstructures. The following analysis is underway to explain the relationship between microstructure features and the formation of spinel oxides.

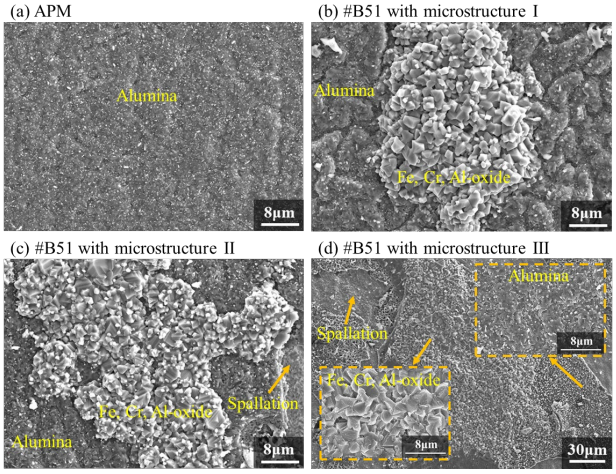

Figure 3. Surface SEM images (SE) of (a) APM and (b)-(d) #B51 with microstructure I-III after the steam oxidation test at 1200 ºC for 2 h

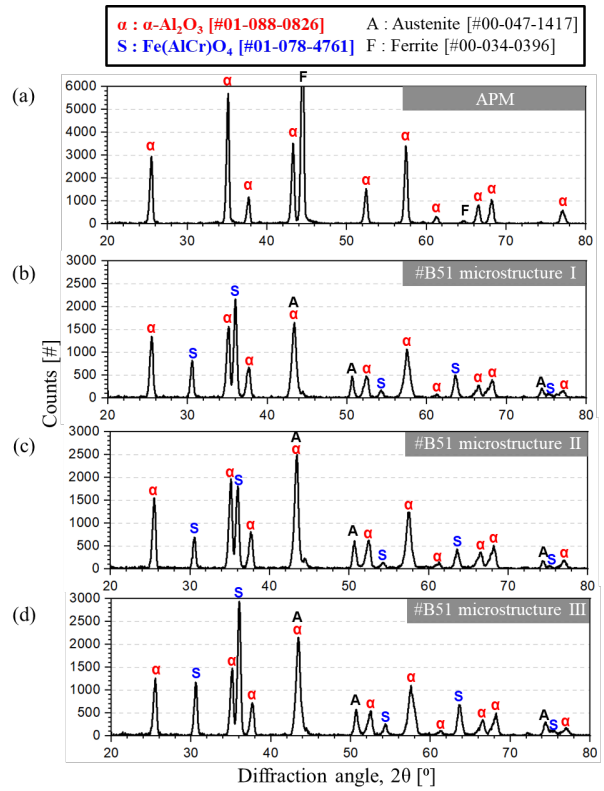

Figure 4. XRD results for (a) APM and (b)-(d) #B51 with microstructure I-III after the steam oxidation test at 1200 ºC for 2 h

4. Summary

High-temperature steam oxidation test at 1200 ºC for 2 h was conducted using ADSS #B51 with different microstructures and APM. Based on the test results and subsequent analyses, the following conclusions were drawn:

- ADSS and APM have very low weight gain in steam test at 1200 ºC. Although ADSS has the same chemical composition, different weight gains were observed in ADSS #B51 depending on microstructures.
- In APM, only α-alumina was formed after the oxidation test. On the other hand, not only α-alumina but also spinel oxides were formed on ADSS #B51
- The relatively fast oxidation rate of ADSS in the early stage results from formation of spinel oxides. The amount of spinel oxides was affected by the existing microstructure of ADSS.
- The following analyses are underway to explain microstructure effect of ADSS on high-temperature oxidation resistance.

Acknowledgement

This study was supported by the MOTIE/KETEP project (No. 20211510100010) of the Republic of Korea.

REFERENCES

[1] B. A. Pint, K. A. Terrani, Y. Yamamoto, and L. L. Snead, Material selection for accident for accident tolerant fuel cladding, Metallurgical and Materials and Transactions E, 2, pp. 190-196, 2015.
[2] K. A. Terrani, Accident tolerant fuel cladding development: Promise, status, and challenges, Journal of Nuclear Materials, 501, pp. 13-30, 2018.
[3] H. Kim, H. Jang, G. O. Subramanian, C. Kim, and C. Jang, Development of alumina-forming duplex stainless steels as accident-tolerant fuel cladding materials for light water reactors, Journal of Nuclear Materials, 507, pp. 1-14, 2018.
[4] C. Kim, H. Kim, C. Jang, K. Kim, Y. Kim, S. Lee, and H. Jang, Feasibility assessment of the alumina-forming duplex stainless steels as accident tolerant fuel cladding materials for light water reactors, International Journal of Energy Research, 44, pp. 8074-8088, 2020.
[5] C. Kim, H. Kim, W. Heo, C. Jang, S. Lee and J. Lee, High-temperature steam oxidation behavior of alumina-forming duplex FeNiCrAl and ferritic FeCrAl alloys at 800 ºC to 1500 ºC, Corrosion Science, 190, 109658, 2021.
[6] R. Prescott and M. J. Graham, The formation of aluminum oxide scales on high-temperature alloys, Oxidation of Metals, 38, pp. 233-254, 1992